EMPIRICAL RADIOMETRIC CORRECTION OF A SILICON PHOTODIODE ROTATING SHADOWBAND PYRANOMETER

JOSEPH J. MICHALSKY†, LEE HARRISON, and BROCK A. LEBARON
Pacific Northwest Laboratory, Richland, WA 99352, U.S.A.

Abstract—We have improved the silicon photodiode-based rotating shadowband pyranometer[1] to suit it for radiometric observations by deriving empirical corrections to mimic thermopile sensors. We present the results of an intercomparison between our rotating shadowband pyranometer and a conventional complement of first-class thermopile instruments. The daily integrated values for total horizontal, diffuse horizontal and direct normal irradiance measured with our rotating shadowband radiometer agree on average to better than 1%, 3%, and 2.5%, respectively, with the thermopile results, after our empirically derived corrections are applied. In absolute units, 10-minute integrated values seldom differ by more than 20 watts/m² from the thermopile values.

1. INTRODUCTION

The most widely used radiation measurement in the solar field is the total incident power per unit area integrated over all wavelengths. Three standard measurements of solar irradiance are the total on a horizontal surface, the diffuse component on a horizontal surface, and the direct normal component with the diffuse excluded.

Traditionally, the preferred instruments in solar radiation measurements have used thermopile detectors. A thermopile responds to temperature differences between two surfaces of greatly differing albedo to which thermocouple junctions are attached. The primary advantage of a thermopile is inherent uniform spectral response across a wide range of wavelengths, depending only on the uniformity of the albedos of the two surfaces.

Modern thermopile radiation sensors are built with temperature-compensating circuits that reduce the error caused by changes in the ambient temperature. The result is a stable and reproducible instrument that has become the workhorse of solar energy measurement. Some of these instruments have received the World Meteorological Organization's first-class rating[2], but typically cost about U.S. $1500.

A field station equipped to measure the diffuse horizontal, total horizontal, and direct normal components of the sun's radiation using currently available instruments will typically use a sun-tracking pyrheliometer and horizontally oriented pyranometer. These two instruments, plus a tracker, plus a data acquisition unit will cost about U.S. $8000. The initial capital costs and the annual maintainance costs associated with such facilities, which can be an appreciable fraction of the capital investment, limit the ability of the solar research community to obtain the climatology needed for resource assessment.

Silicon cell-based sensors are now used for pyranometric measurements[3]. These sensors are very stable and rugged and experience typical sensitivity degradation of less than 2% per year even in reasonably harsh environments. Another advantage of these sensors in some applications is their short response time of about 10 microseconds. However, their cost, which is 10% to 20% that of thermopile instruments, is their most attractive feature.

Photometry is an application where a silicon detector is inherently the better choice. Photometers are designed to have the same spectral response as the average human eye. The eye's response peaks at 550 nm and falls to near zero around 400 and 700 nm. This wavelength range is well within the sensitivity of silicon, and temperature and cosine effects are minimal in this spectral region. Photometry was the original application for which we developed the rotating shadowband photometer[1].

A detailed description of our rotating shadowband instrument appears in [1]. Briefly, it is a photometric, computer-controlled shadowband pyranometer. Once each time period (typically, a minute), the total irradiance is measured, and then the band moves into position to block the direct beam for the diffuse measurement. The band is positioned by stepping precisely to the calculated solar hour angle. Additional measurements are made with the band in proximity to, and on either side of, the sun to permit a real-time correction for the effect of the shadowband's obstruction of, what can be, an appreciable fraction of the diffuse radiation during the diffuse measurement. The direct beam radiation is calculated from the difference in these two measured quantities and the cosine of the solar zenith angle.

Solar photometry serves a limited audience. Architects and daylighting engineers use this infor-

---

† Member of ISES. Present address: Atmospheric Sciences Research Center, State University of New York at Albany, Albany, NY 12222

mation, but there are many more potential users of radiometric data. For example, while an architect needs photometric information to size windows for particular tasks, he requires the bolometric quantity to calculate heat gain through the same windows. Moreover, most solar thermal applications are not wavelength specific, i.e., any input energy regardless of wavelength is useful.

Why not use a thermopile pyranometer in the rotating shadowband device? This is a possibility, but there are two reasons why we did not start with this approach. We are trying to develop an instrument whose total cost approaches that of one first-class pyranometer. The other reason is the thermopile's time constant. Shading times need to be long in order to make proper measurements. This adds to the time between diffuse and total horizontal measurements that could cause errors in the calculated direct normal if cloud conditions change rapidly.

In this paper we discuss the limitations of silicon photodiodes in performing irradiance measurements traditionally made with thermopiles, our instrumentation to separate the diffuse and direct beam components, and correction procedures that improve the intercomparability of the two methods. We finish with examples of our corrected output in comparison to first-class equipment and describe our plans for future device development. We believe that our instrument can replace the more expensive bolometric instruments in many applications and permit researchers to obtain data more reliably.

2. LIMITATIONS OF SILICON PERFORMANCE IN A RADIOMETRIC APPLICATION

If we wish to use a photodiode to make a bolometric measurement, wavelength response and spectral distribution become significant problems. The photodiode wavelength response is not uniform, nor is it sufficiently broad to encompass all the solar wavelengths transmitted by the atmosphere. A second-order problem with silicon is its dependence on temperature. Finally, as is the case with all pyranometric detectors, even thermopiles, silicon cell pyranometers must be corrected for their cosine response at high angles of incidence.

The first-order variation of current with temperature is removed if a silicon photodiode is operated with zero potential difference. However, there persists a significant temperature sensitivity at both the ultraviolet and infrared limits of the detector[4]. If uncorrected, this may cause a change in sensitivity of about 5% from winter to summer given a temperature range typical of mid-latitudes.

Silicon cell pyranometers are usually built with the photodiode placed beneath a diffusing disk designed to improve the cosine angular response of the instrument. (A perfect cosine response would mean that a planar hemispherical field-of-view re-

ceiver's response to a constant, parallel source of radiation would vary as the cosine of the angle between the normal to the plane of the receiver and the direction of the source.) The disk is usually shaped to compensate for the specular reflectance at large incident angles. This shape correction performs well for wavelengths below 800 nm, but, according to some unpublished work of the resource assessment branch at the Solar Energy Research Institute in Golden, Colorado, some diffusers become somewhat transparent and, consequently, fail at longer wavelengths.

Photodiodes and thermopiles make fundamentally different measurements. A photodiode counts the arrival of photons with an energy greater than the diode band-gap. The photon energy in excess of the band-gap is dissipated as heat and is not measured. A thermopile measures power, and thus the measurement integral over wavelength represents the first moment of the photon spectral distribution. This relationship gives rise to spectral response characteristics that complicate the problem of interrelating the two measurements.

If the solar spectra presented to the detector were qualitatively invariant, i.e., exhibiting the same relative spectral distribution at all times, then the silicon detector's spectral characteristic would be unimportant. However, the spectral shape for the total horizontal irradiance changes with air mass and cloud cover. The change is more significant for the direct normal component of the irradiance and so large for the diffuse that uncorrected measurements can approach 40% error. Reducing these errors is necessary before a photodiode can make acceptable surrogate measurements in place of a bolometric instrument.

3. MECHANICAL AND ELECTRONIC SHADOWBAND IMPROVEMENTS

We have undertaken a substantial effort to improve utility and reliability, and to reduce mechanical and electronic sources of error. In large measure this has simply been the normal result of diagnosing and designing fixes for problems discovered during our preliminary experiments. These efforts have resulted in a substantially improved device.

At times the prototype shadowband became misaligned after tracking well for long periods. The problem was traced to metal fatigue at the attachment of the motor housing to its support, presumed caused by wind-driven oscillations. After reinforcement we have had no further difficulties.

We have improved the accuracy of our geared stepper motor and are considering the use of either direct-drive micro-steppers or dc motor tachometers. These further changes are being pursued only for their potential cost and power reductions: We feel that the angular accuracy we currently achieve is adequate.

The data acquisition and control system is one-half its former size and requires much less power. The operating system and applications program are resident on PROM. There are 24 kilobytes of battery-backed RAM memory, of which 22K are available for data storage. (The remainder is consumed by program variables and buffer space.) With the battery-backup the system will automatically restart when repowered after an outage, without losing either the time or stored data. The operating system is completely different and is much more flexible with regard to accommodating new applications.

One of the most significant improvements has been to improve the analog to digital conversion quantization from 8-bits to 12-bits. This means that the output of the pyranometer can be adjusted such that even dark overcast skies are measured with a 1% digitization accuracy. There are 64 multiplexed analog inputs available: This number is much larger than required, but allows future expansion and permits the system to collect any ancillary measurements made at the site.

One analog input is used to measure the voltage drop across a calibrated thermistor affixed to the silicon photodiode. This arrangement permits temperature-dependent corrections to be applied.

The improvements in hardware and operating software have allowed us to increase the rotation speed to one sample every 30 seconds. At this rate we see little evidence of differences between instruments that are sampling out of phase by as much as 20 seconds. This observation allays a concern that rapidly moving clouds could significantly affect the measured signals while the measurement is in progress. Our technique requires a short delay between the total and diffuse horizontal measurements that are used to calculate direct beam irradiance. This delay appears to cause no detectible error given averaging periods of 10 minutes or longer.

4. EMPIRICAL CORRECTIONS

We routinely operate a pyranometer and a pyrheliometer that have a first-class rating for the measurement of solar radiation from the World Meteorological Organization[2]. It was our original intention to use an active cavity pyrheliometer[5] to carefully calibrate the pyrheliometer and then the pyranometer using the shading disk technique[6] in order to improve the existing calibrations. (Both instruments were previously calibrated in an extensive side-by-side comparison by Ed Flowers at the NOAA solar radiation calibration facility in Boulder, Colorado.)

Our attempts to calibrate using the shading disk method indicated a few percent change in calibration constant with solar-zenith angle. Realizing the magnitude of the additional effort to calibrate as a function of solar zenith angle and our limited re-

sources, we elected to accept the calibration constants that had been derived independently. All of our attempts to match the thermopile and silicon cell instruments accept the existing thermopile calibrations as absolute despite our understanding that they are somewhat solar angle dependent. The purpose of this paper then is to demonstrate how well first-class instrumentation can be mimicked by silicon cells. If we were to develop our corrections against absolute standards, we could, presumably, derive even better corrections than we will demonstrate in the following paragraphs.

When the total wavelength range of the silicon photodiode is used as in the radiometric application we are now considering, the detector sensitivity will depend on the temperature at which it is used. In general, the warmer the diode the more sensitive it is to the normal solar spectrum. The blue response decreases with increasing temperature, but the red response increases and dominates[4].

A common method for eliminating temperature dependencies is to hold the photodiode at a constant elevated temperature. Instead, we decided to measure the temperature sensitivity of the device and make temperature corrections. Doing so is less expensive and requires less power.

We began by operating two silicon cell pyranometers side-by-side with calibration constants adjusted to give the same irradiances at the outset of the measurements. We then heated one pyranometer and formed the ratio of the two as we increased the temperature to 40°C. We then allowed it to cool to ambient continuing our 30-second measurements. We then further cooled the same pyranometer to −6°C and allowed it to warm to ambient. The points during heating are plotted in Fig. 1 with closed circles and the cooling phases are plotted as open circles. The sensitivity is nearly linear with temperature, and corrections can be made to about 0.7%. The test illustrates some hysteresis in the recovery phases, which we attribute to the thermistor and sensor not being in thermal equilibrium because of the rapid cooling and heating. These rates were greater than would naturally occur.

Consider a clear day measurement of the total horizontal irradiance: At low sun angles (high air mass) the irradiation both changes its spectral character and assumes incidence angles where the cosine sensitivity may need correction. Since spectral and cosine response problems are often intertwined, we decided not to try to correct them separately.

We begin by deriving a calibration for the total or global irradiance. A scatter plot of total horizontal as measured by the silicon cell (tots) to the total horizontal as measured by the thermopile (tott) appears in Fig. 2 along with the equation representing a linear least squares fit to the data. The data points are 10-minute averages taken from 18 days with a fair mix of cloudy and clear periods in late August and early September. A 45° line indi-
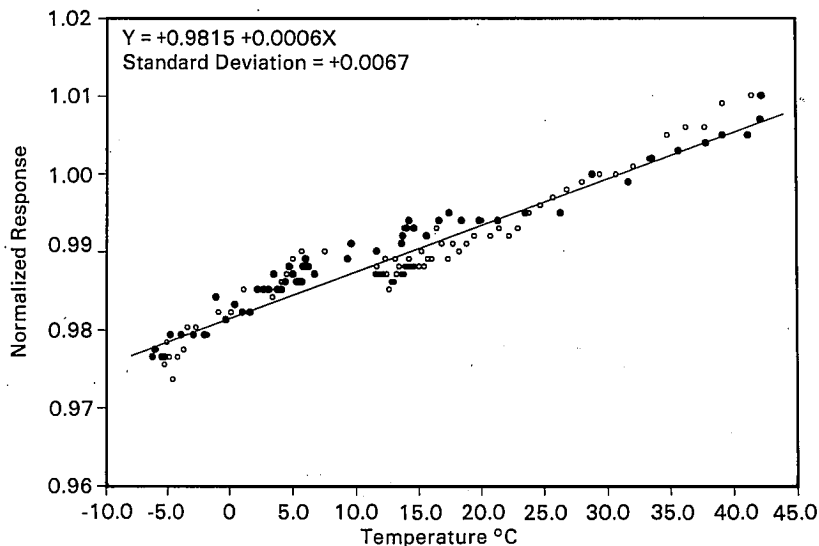
Fig. 1. Ratio of temperature moderated silicon cell to ambient temperature cell versus temperature. Closed circles are heating phases and open circles are cooling phases.

cating perfect correlation is shown for reference. Our first correction of the data was to find the best calibration constant for the silicon cell pyranometer from a linear least squares fit. The outcome from this procedure appears in Fig. 2. The constant that multiplies tott is very close to 1. However, if we examine Fig. 2 closely, we notice that relative to the 45° line, the data are low at the high and low irradiances and high at the mid-value irradiances. We tentatively attribute this to a slight nonlinearity in either the silicon cell response or the thermopile response. A plot of the ratio tots/tott versus tots as given in Fig. 3 shows this more clearly. (In this and in all of the following figures involving the ratio of two irradiances we exclude values taken for zenith angles greater than 80°, i.e., we do not derive corrections that include very high air masses, since they contribute little insolation, and they distort the derived corrections.) The fit to the data is a least squares fit of

$$tots/tott = a + b * \ln(tots) + c * [\ln(tots)]**2. \quad (1)$$

Applying this correction to the tots data (dividing tots by the right-hand side of eqn (1)) and replotting on the same coordinates, we have the results shown in Fig. 4. Most scatter is at very low irradiances. From the fit drawn through the data and the coefficients of the fitting equation, it is apparent that the ratio of the two total horizontal measurements is close to one for all cloud conditions. Figure 5 is the scatter plot of tots versus tott after applying the correction. From the plot it is clear that we have improved the fit for all values of irradiance. The slope is close to one and the y intercept is near zero. The small cluster near zero irradiance are points where tots was less than 20 watts/m². The severity of the corrections for these low values often produced unreasonable results and, consequently, were not applied below this value.

We next focused our attention on the diffuse correction, which we anticipated would be somewhat less satisfactory. The thermopile diffuse horizontal irradiance is calculated by differencing the total horizontal irradiance and the direct horizontal irradiance. The latter is obtained by multiplying the direct normal irradiance by the cosine of the solar
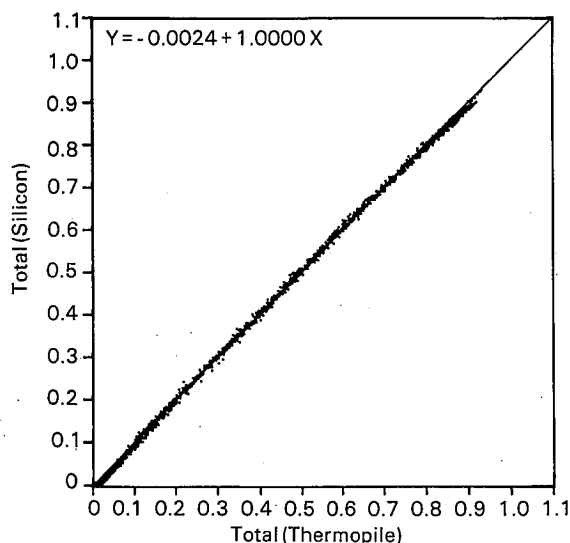

Fig. 2. Total horizontal irradiance measured by silicon photodiode versus that quantity measured by thermopile. Equation resulting from least squares fit. Line drawn through data represents perfect correlation.
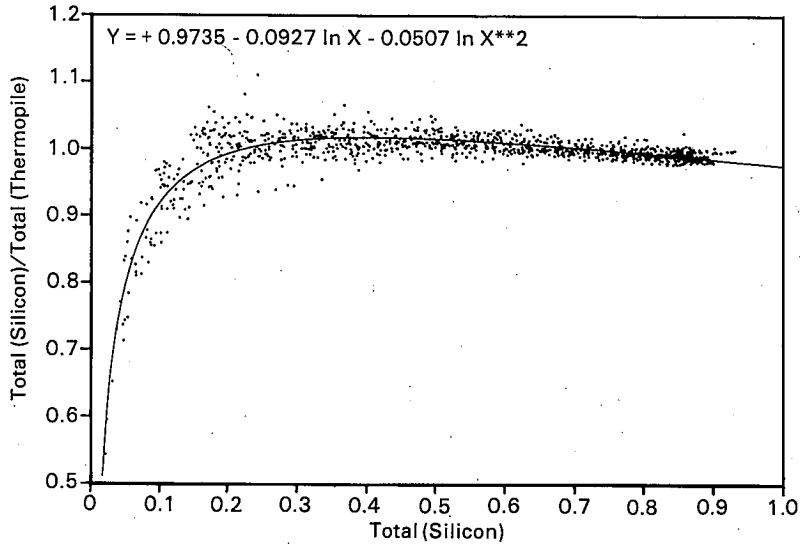
Fig. 3. Ratio of total horizontal irradiance measured by silicon to that quantity measured by thermopile versus silicon measurement. Equation and curve resulting from least squares fit.

zenith angle. A scatter plot of the silicon cell diffuse (difs) versus the thermopile diffuse (dift) appears in Fig. 6. The data are somewhat skew with respect to the 45° line, which represents perfect correlation, but the difficult to judge, and more serious, problem is for low irradiances where most of the clear day values occurs.

To better see this, we plot the data in a form suggested by LI-COR in the correction of their silicon cell shadowband pyranometer[7]. Figure 7 is a plot of the ratio of difs to dift versus difs/tots (a cloudiness index). We tested other variables such as diffuse-to-direct and direct-to-total ratios, but

the diffuse-to-total ratio provided the least scatter in the diffuse corrections that follow. This plot confirms our physical insight about the response of silicon to diffuse. The left side of the plot represents clear conditions. The diffuse irradiance measured in this case is that of clear blue sky whose spectral distribution peaks in the least sensitive region of the photodiode sensitivity. As cloudiness increases (the right-hand side of the plot), the diffuse irradiance takes on a spectral distribution similar to the one under which the silicon cell pyranometer was calibrated, and, consequently, the ratio is closer to one. A least squares fit to an equation of the same
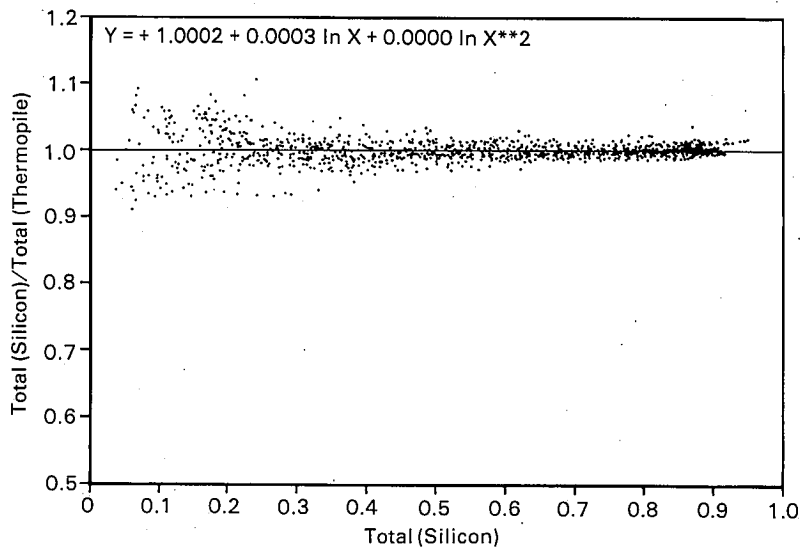

Fig. 4. Same as Fig. 3 after correction by equation derived in that figure.
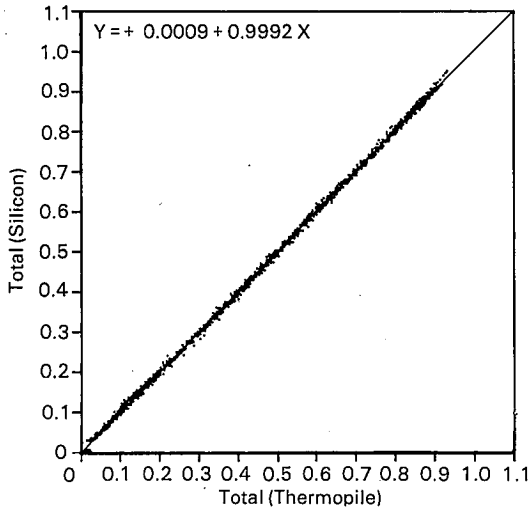
J. J. MICHALSKY *et al.*

Fig. 5. Same as Fig. 2 after correction in Fig. 3 is applied. Note improvement over Fig. 2 at all irradiance levels.
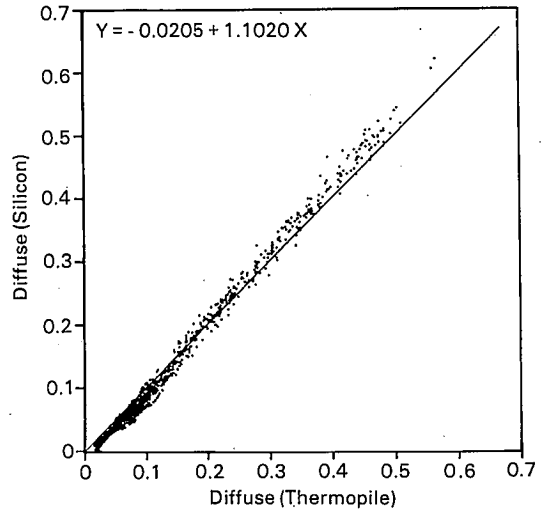
Fig. 6. Diffuse horizontal irradiance measured by silicon versus that quantity measured by thermopile. Equation resulting from least square fit. Line drawn through data represents perfect correlation.
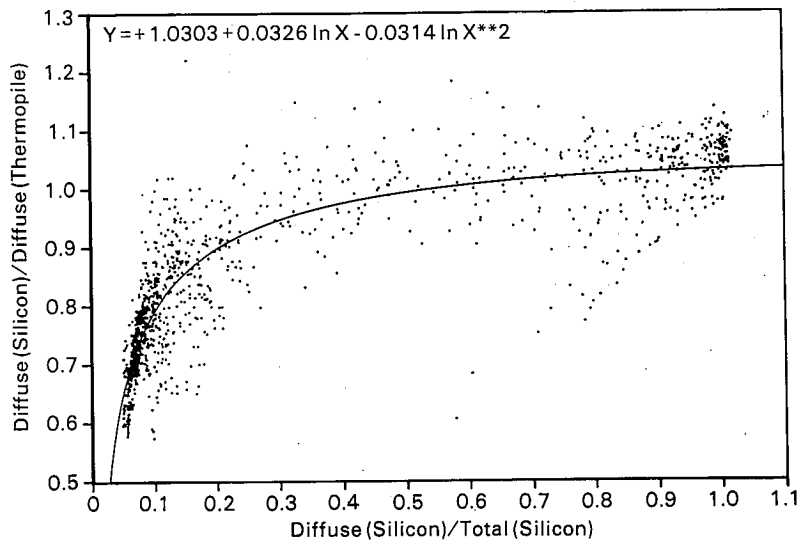

Fig. 7. Ratio of diffuse horizontal irradiance measured by silicon photodiode to that quantity measured by thermopile versus the ratio of diffuse as measured by silicon to total horizontal as measured by silicon. Equation and curve resulting from least squares fit.

functional form as in eqn (1) was performed, i.e.,

$$difs/dift = a + b * \ln(difs/tots)$$
$$+ c * [\ln(difs/tots)]**2. \quad (2)$$

The fit seems reasonable and the shape is much like the LI-COR[7] fit. There is more scatter than in the LI-COR data because, perhaps, we are using 10-minute (as opposed to hourly) values. The extremely divergent points in the lower right portion of the plot are associated with ratios of extremely low irradiance values. Figure 8 is the same plot after correction using the derived fit. The fit and the coef-

ficients of the regression both indicate that the ratio is near one for all cloudiness levels.

Figure 9 is a scatter plot of the corrected silicon cell diffuse versus the thermopile diffuse. Again we have drawn a 45° line for comparison. The slope is apparent in the data and in the coefficients of the linear least squares fit. The results corrected using the least squares coefficients to a linear fit from Fig. 9 appear in Fig. 10. The improvement in visual fit and coefficients is readily apparent.

Our final corrections were to the direct beam irradiance. A scatter plot of the silicon cell direct (dirs) versus the thermopile direct (dirt) appears in

Fig. 11. Again the 45° line is drawn. The poor agreement is obvious in the plot and in the regression coefficients. Earlier we found that at high and intermediate irradiance silicon cell diffuse is underestimated. One step in determining the silicon cell direct is subtracting diffuse from total horizontal irradiance. This step yields silicon cell direct values that are too high relative to the thermopile direct, as seen in Fig. 11. After considering several approaches to improving these data, we elected to separately fit silicon cell direct irradiances above and below 480 watts/m^2 (as measured by silicon) with linear regressions. The corrected dirs versus dirt appears in Fig. 12. The scatter is larger than in the total horizontal case and comparable to the dif-

fuse. The overall improvement in fit is clearly shown by both the plot and the regression coefficients.

The largest scatter occurs at mid-range. Values in this range can arise from high air mass clear conditions and low air mass partly cloudy conditions. Since the partly cloudy diffuse spectrum is similar to the spectral distribution used to calibrate the cell, little correction is required. However, considerable correction is needed, as we have shown, for clear sky conditions. In trying to achieve an average correction, the partly cloudy sky diffuse is overcorrected, and the clear sky diffuse is undercorrected. Applying an average correction has the opposite effect, of course, on direct values. This will be quite
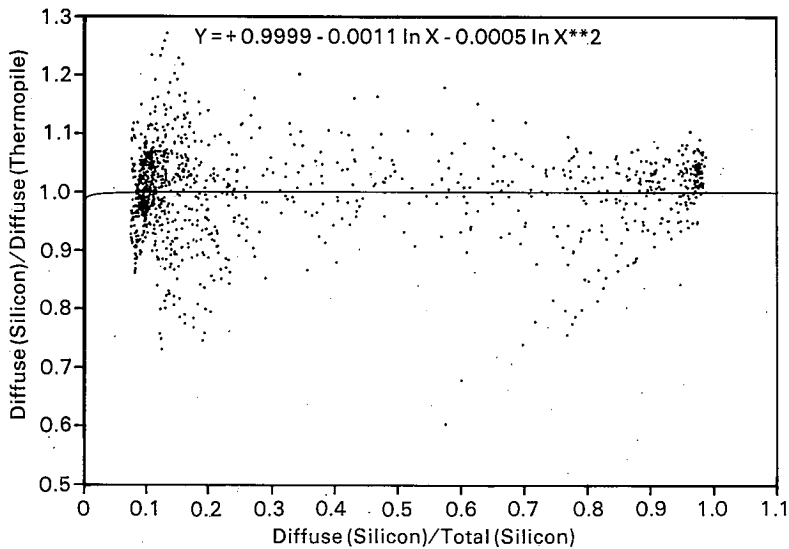

Fig. 8. Same as Fig. 7 after correction by equation derived in that figure.
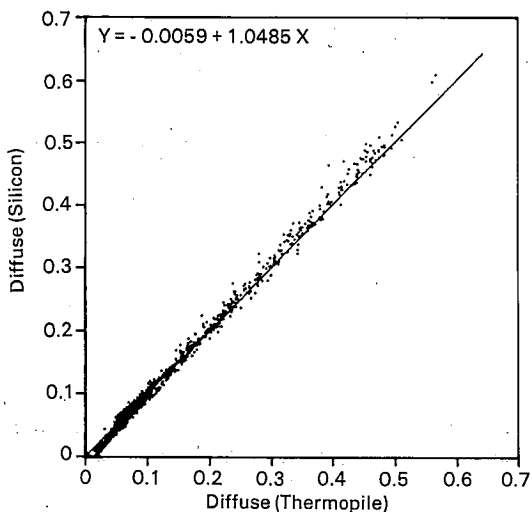

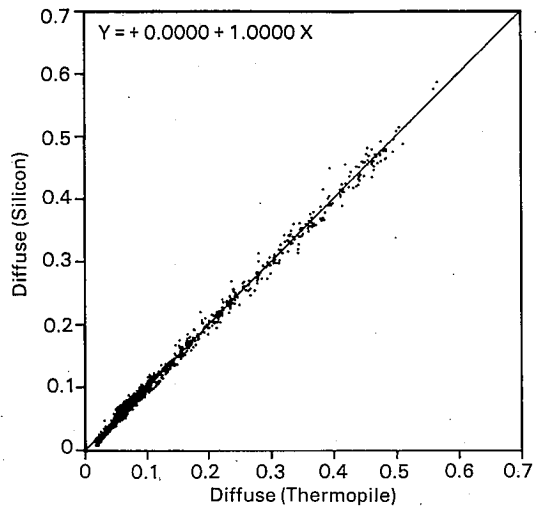Fig. 9. Same as Fig. 6 after correction in Fig. 7 applied.

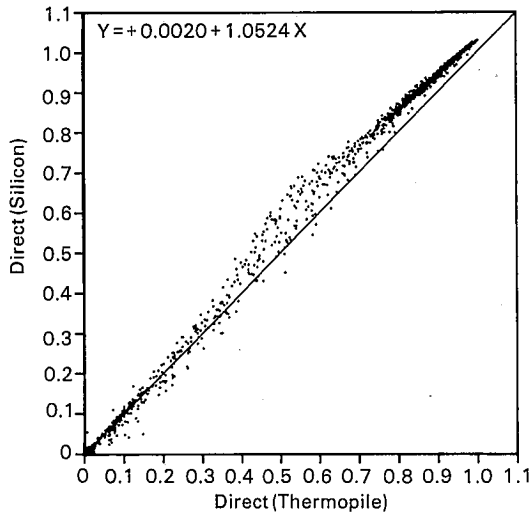Fig. 10. Same as Fig. 9 after correction by equation derived in that figure.

Fig. 11. Direct normal irradiance measured by silicon photodiode versus that quantity measured by a thermopile. Equation resulting from linear least squares fit. Line drawn through data represents perfect correlation.
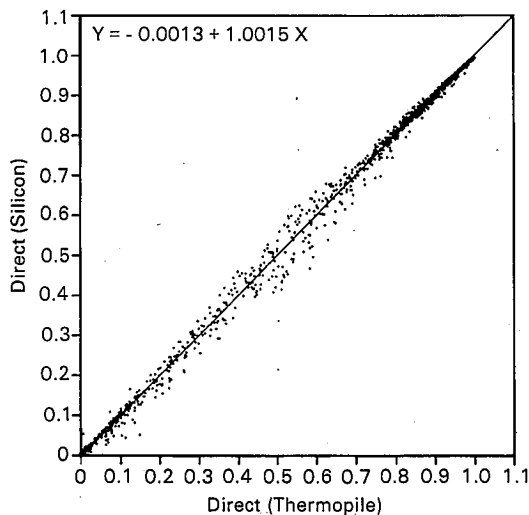

Fig. 12. Same as Fig. 11 after corrections applied.

evident in the direct as we shall see in the examples to follow in the next section.

5. RESULTS AND CONCLUSIONS

In this final section we will compare the output of first-class instrumentation with corrected silicon cell output on both a cloudy and a clear day. All plots are of the total horizontal, the diffuse horizontal and the direct normal irradiances as measured by the silicon cell rotating shadowband radiometer and the thermopile instruments.

The plots of both clear and cloudy days will

allow a comparison of each component throughout the day with 10-minute resolution. The differences in percent between summed daily components obtained by

$$\%\text{diff} = ((\text{xxx}s - \text{xxx}t)/\text{xxx}t) * 100, \qquad (3)$$

where xxx is either tot, dif or dir, are given. These are neither the best of the days nor the worst, but should be considered typical. The best and the worst, however, do not differ appreciably from these plots.

Figure 13 is a plot of clear day irradiances in late summer before (a) and after (b) correction. The total irradiances, after correction, track extremely well throughout most of the day with the largest disagreement near noon amounting to less than 2%. This is about 15 watts/m² in absolute units. The integrated total horizontal values for the day agree to better than 1%. The diffuse horizontal irradiances have about the same absolute discrepancy where the differences are largest, but this translates into a much larger fractional difference, since the diffuse is much smaller than total horizontal on clear days. The daily integrated values of diffuse horizontal irradiance, nevertheless, agree to better than 5%. The clear day case is expected to be the worst one for intercomparison of the diffuse component.

The daily integrated values of direct beam irradiances agree best on clear days. We have noted the early morning and late afternoon discrepancies on several occasions, and we attribute it to the undercorrection of diffuse at high air mass as explained in the last section. Note that the silicon direct is too high. Despite this discrepancy, the daily direct beam integrated values agree to better than 1%.

On the partly cloudy day in Fig. 14 most of the absolute discrepancies, after correction, are less than 20 watts/m². Since the direct is smaller on cloudy days than on clear, the daily integrated value can have a larger fractional error, but is usually less than 3%. The diffuse irradiance values are generally in better agreement on cloudy days because they are larger in an absolute sense and because the spectral distribution is more nearly that under which the device is calibrated. Note that the "correction" of the cloudy portion of the direct plot actually produces somewhat poorer agreement for the reason stated in the last section, i.e., the direct is overcorrected.

As a resource assessment tool, the corrected device appears to be capable of matching average thermopile measurements of daily insolation to better than 1% for total horizontal, 2.5% for direct beam, and 3% for diffuse horizontal. Typical, maximum deviations of 10-minute irradiances were about 20 watts/m², which along with the plots indicate that hourly values should not be too much worse than the daily total errors.
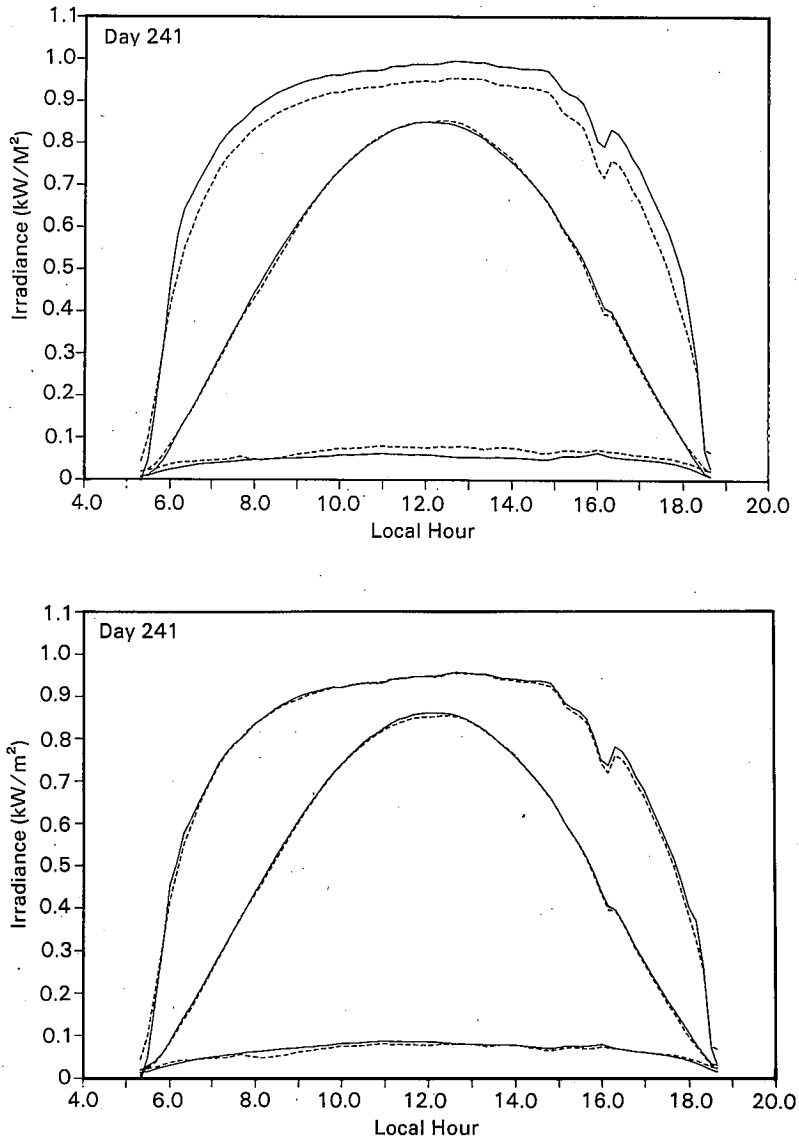
Fig. 13. Direct normal (top), total horizontal (middle), and diffuse horizontal irradiances measured by silicon photodiode (solid) and thermopile (dashed) on clear late August day. 13(a) is before correction and 13(b) is after.

We wish to reiterate that our tests are a comparison of devices whose absolute calibrations exhibit comparable errors. If we could routinely calibrate against absolute standards, then our absolute accuracies may in fact closely match first-class instrumentation accuracies.

Our instrument could satisfy a multitude of medium accuracy resource assessment needs at a capital cost well below that of first-class instruments. The savings would be even larger when maintenance and calibration expenses are considered.

6. FUTURE WORK

A logical next step is to adapt this device for remote applications where no line power is available. Almost all of the electronics are low-powered CMOS parts. The largest power consumption oc-

curs in running the stepping motor. As presently configured the instrument could run for one or two months using an automobile lead-acid battery and a "no wasted motion" algorithm. This power consumption could also be met by a modest solar cell array of approximately 0.2 m². Development of a dc motor and tachometer feed-back control should reduce the power consumption further.

Under consideration for the next major modification of this device is the development of a spectral radiometer, i.e., one with low spectral resolution operated, perhaps, in a parallel mode such that spectral elements are sampled simultaneously. This device would be of value to photovoltaic resource assessment; permit a better correction of spectral response for pyranometric measurement; and aid atmospheric scientists with a new, low-cost tool for
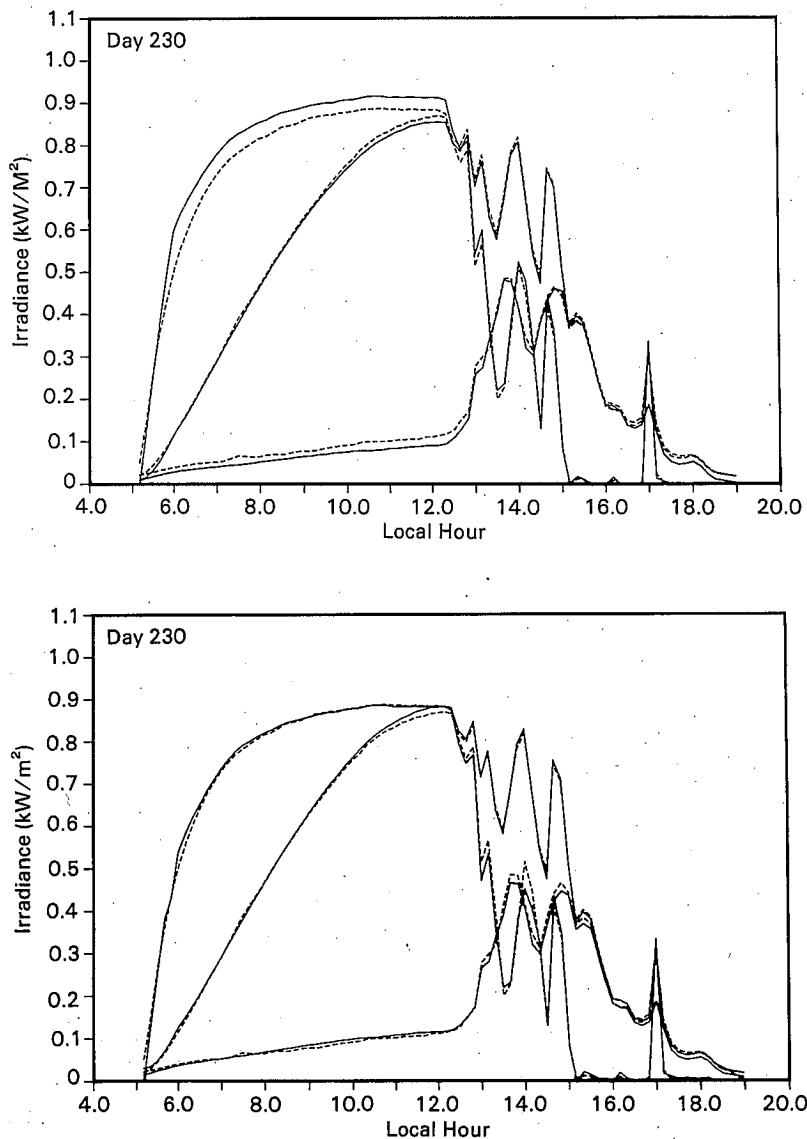
Fig. 14. Same as Fig. 13, except the day is partly cloudy. The three irradiances may be followed in the afternoon by noting that in the morning the order is the same as it was in Fig. 13.

spectrally detailed aerosol and trace gas measurements.

REFERENCES

1. J. J. Michalsky, J. L. Berndt and G. J. Schuster, A microprocessor-based rotating shadowband radiometer. *Solar Energy* **36**, 465–470 (1986).
2. K. L. Coulson and Y. Howell, Solar radiation instruments. *Sunworld* **4**, 87–94 (1980).
3. J. P. Kerr, G. W. Thurtell and C. B. Tanner, An integrating pyranometer for climatological observer stations and mesoscale networks. *J. Appl. Meteorol.* **6**, 688–694 (1967).
4. EG&G Electro-Optics, Silicon photovoltaic detectors and detector/amplifier combinations. Application Notes D3011C-5, Salem, Massachuetts, USA (1981).
5. J. M. Kendall and C. M. Berdahl, Two blackbody radiometers of high accuracy. *Appl. Opt.* **9**, 1082–1091 (1970).
6. M. Iqbal, *An Introduction to Solar Radiation.* Academic Press, Toronto (1983).
7. LI-COR, Inc., 2010 miniature shadow band instruction manual. Publication No. 8105-22, Lincoln, Nebraska, USA (1981).